Proceedings of the 1996 IEEE
International Conference on Robotics and Automation
Minneapolis, Minnesota - April 1996

Stability of Control System in Handling of a Flexible Object by Rigid Arm Robots

T. Yukawa*1 M. Uchiyama*1 D. N. Nenchev*1 H. Inooka*2
*1 Dept. of Aeronautics and Space Engineering, Tohoku University
*2 Graduate School of Information Sciences, Tohoku University
Aramaki-aza-Aoba, Aoba-ku, Sendai 980–77, JAPAN

Abstract

In this paper, we deal with the handling of a flexible object by rigid arm robots. We consider three main tasks: first, to propose a mathematical model for a variety of flexible objects of our daily life; second, to design a controller to achieve cooperative handling of the flexible object by the robots; and third, to analyze the stability and robustness of the control system. In particular, in space, it seems that demands for manipulating a large-scale structure by a space robot will be increasing. Therefore, it is important to constitute the cooperative control problem of several robots handling a flexible object, and to analyze the proposed control system.

1 Introduction

The control problem for handling a flexible object by several robots is more complex than that of handling a rigid object [1]. This is because there is no information about the internal potential in the flexible object. There is no one-to-one relation between the input forces from the robot and the reaction forces at any point on the object. The position sensors mounted on the robots cannot observe the deflection at every point of the flexible object, except for the handling points. The force/torque sensors mounted on the robots cannot also estimate the force/torque being generated at any point of the flexible object, except for the handling points. As a result, vibration, spill over and destabilization occur.

Nakagaki *et al* [2] have realized the position control of a flexible object handled by a rigid robot, using the static shape function of the object. Their purpose was to insert one end of the flexible object into a hole while holding the other end. In our previous work [3], we have constituted a new control system to achieve two performances simultaneously, *i.e.*, following up one end of the flexible object and its vibration suppression by a robot.

Recently, some researchers have started the study of control of a flexible object using a dual-arm robot. Zheng *et al* [4], [5], [6] and Kosuge *et al* [7] have realized cooperative position control of the flexible object while utilizing the mathematical modeling on the static bending function of the flexible object. Svinin *et al* [8], [9] have applied geometrical analysis to perform position control and vibration suppression of the flexible object. The flexible object has been modeled as a system of lumped masses and springs.

On the contrary, we have designed a control system to realize active handling of a vibrating flexible object [10]. The aim of our work was to realize position control of the flexible object while suppressing its vibration using a dual-arm robot. For this purpose, we have proposed a model for the system connecting the robots and the object, so as to guarantee the whole system's stability. However, we did not consider the dynamical characteristics of the flexible object.

In this paper, we use a dynamical model of the flexible object. The dynamics of the flexible object cannot be neglected. If the parameters of the object are larger than that of the robots, it is important to consider the relationship between the dynamics of the robots and the object. We also expand the dimension of vibration from 1-D space, as in the paper [10], to 2-D space. This object can be transformed in 2-D space, and the dynamics of the body itself becomes of very complex mathematical structure. This model covers a number of flexible objects, from daily life: *e.g.*, bean curds, cakes, as well as spiral wires as shown in Figure 1.

The design of cooperative control for the robots and the dynamic flexible object makes it possible for a micro robot to manipulate a macro object while satisfying the stability of the control system. Finally, we also propose a discrimination criterion about the stability and analyze the robustness of the control system.

0-7803-2988-4/96 $4.00 © 1996 IEEE

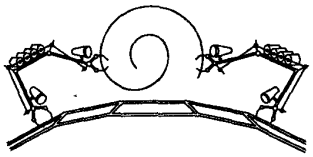

Figure 1: Situation of handling a wire by two robots.

2 Problem formulation

To simplify the problem, we consider motion in 2-D space. We suppose that the characteristics of both the robots and the object are already known. Suppose also that a set of robots have grasped the object, while another set of robots are supporting it just through point contacts without generating any force/torque. In this research, except for the multiple-arm robot used in subsection 4.2, we deal with a dual-arm robot equipped with end-effectors. To be more specific, we consider the problem that the dual-arm robot moves to the reference position/posture having grasped the object, and suppressing in the same time its vibration. Such a situation may occur when two robots handle a flexible structure in space (Figure 2).

3 Kinematics and dynamics

3.1 Equation of motion of the rigid robot

Using Lagrange's formulation, the equations of motion represented as first order differential equations in state-space, with the state-space vector $\boldsymbol{\Theta}_{L,R} = [\boldsymbol{\theta}_{L,R}^T \ \dot{\boldsymbol{\theta}}_{L,R}^T]^T$, are written as follows:

$$\dot{\boldsymbol{\Theta}}_{L,R} = \boldsymbol{A}_{L,R}\boldsymbol{\Theta}_{L,R} + \boldsymbol{B}_{L,R}\boldsymbol{\tau}_{L,R} + \boldsymbol{W}_{L,R} \quad (1)$$

where $\boldsymbol{\theta}_{L,R} \in \Re^{3\times 1}$ are the joint angle vectors, $\boldsymbol{\tau}_{L,R} \in \Re^{3\times 1}$ are the torque input vectors, and $\boldsymbol{W}_{L,R} \in \Re^{3\times 1}$ are the non-linear terms. The symbols L and R stand for the "Left" arm and the "Right" arm, respectively. The gravity term has been neglected since we consider application in space.

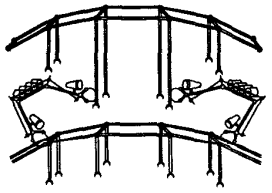

Figure 2: Two space robots handling a flexible structure.

3.2 Modeling of the object

We consider the flexible object to be a beam which is grasped by the robots, such that its ends are free. While the robots handle the object, they have to suppress its vibration, and furthermore to control its deformation.

The model of the object has constraint density and mass distribution. We have studied the handling of a flexible object which is vibrating in 1-D space only, as mentioned in Section 1 [10]. In this paper, we deal with a beam whose characteristics of motion are in 2-D space. That is, the dynamic beam moves flabby in vertical and horizontal directions. The situation of a flying flexible object while vibrating is shown in Figure 3. The object can be expressed by a mathematical model, even if its external appearance forms a spiral or a closed curve.

3.2.1 Distributed and finite dimensional model of the object

Let's derive the equation of motion of the object using a method proposed by Simo [11], which reveals the construction and expansion in 2-D space. Figure 4 shows the bending displacement of a small element geometrically.

Define a universe coordinate system $\Sigma(\boldsymbol{e}_1, \boldsymbol{e}_2)$, and a small element coordinate system $\Sigma'(\boldsymbol{e}_1', \boldsymbol{e}_2')$. For the small element at $x = x_0$ parallel to direction $\boldsymbol{e}_1$, define the tiny expansion length parallel to direction $\boldsymbol{e}_1$ to be $\tilde{x}$, the tiny expansion length parallel to direction $\boldsymbol{e}_2$ to be $\tilde{y}$, and the tiny angle between the elements to be θ, respectively. Setting the elements $\tilde{x}$, $\tilde{y}$ and θ as the state-space variable of the system, the equation of motion is given by:

$$A_\rho \ddot{\boldsymbol{\phi}}_0 + \mu A_\rho \dot{\boldsymbol{\phi}}_0 - \frac{\partial \boldsymbol{B}_0}{\partial x_0} = \boldsymbol{n} \quad (2)$$

$$I_\rho \ddot{\theta} + \mu I_\rho \dot{\theta} - J_\theta - \boldsymbol{J}_0 \boldsymbol{B}_0 = m \quad (3)$$

where the state-space variables are $\boldsymbol{\phi}_0 = \{x_0 + \tilde{x}(x_0, t)\}\boldsymbol{e}_1 + \tilde{y}(x_0, t)\boldsymbol{e}_2$ and $\theta = \theta(x_0, t)$. $A_\rho = A_\rho(x_0)$ and $I_\rho = I_\rho(x_0)$ are the inertial force coefficients, h is

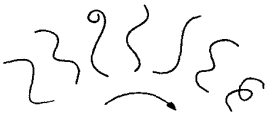

Figure 3: Flying flexible object in 2-D space.

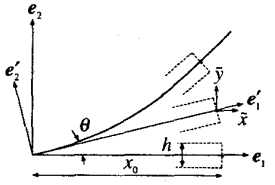

Figure 4: Element of the flexible object.

the width, μ is the damping force coefficient in proportion to $\dot{\phi}_0$, and $\dot{\theta}$. $\boldsymbol{n} = n_x(x_0,t)\boldsymbol{e}_1 + n_y(x_0,t)\boldsymbol{e}_2$ is a vector consisting of the external force n_x in a component of direction $\boldsymbol{e}_1$, and the external force n_y in a component of direction $\boldsymbol{e}_2$. $m = m(x_0,t)$ is the external moment input, and $\boldsymbol{B}_0 = \boldsymbol{B}_0(\boldsymbol{R}_0(\theta), \tilde{x}, \tilde{y}, \theta)$, $J_\theta = J_\theta(\theta)$, $\boldsymbol{J}_0 = \boldsymbol{J}_0(\tilde{x}, \tilde{y})$. $\boldsymbol{R}_0$ is the transformation matrix from the coordinate Σ to the coordinate Σ'.

Set the state-space variable as $\boldsymbol{x}_b(x_0,t) = [x_0 + \tilde{x}(x_0,t)\ \tilde{y}(x_0,t)\ \theta(x_0,t)]^T$, and the control input as $\boldsymbol{u}_b(x_0,t)=[\boldsymbol{n}^T\ m]^T$. From eqs. (2), (3), the equation of motion of the flexible object is given as follows:

$$\boldsymbol{A}_b\ddot{\boldsymbol{x}}_b(x_0,t) + \boldsymbol{B}_b\dot{\boldsymbol{x}}_b(x_0,t) + \boldsymbol{W}_b(\boldsymbol{x}_b(x_0,t)) = \boldsymbol{u}_b(x_0,t) \tag{4}$$

which is a distributed parameter system.

Setting again the state-space as the position and posture $\boldsymbol{x}_{bf}(t) = [x_1\ y_1\ \theta_1\ \cdots\ x_n\ y_n\ \theta_n]^T\ \ (n < \infty)$, from the distributed parameter system eq. (4) we obtain an approximated finite dimensional system using the mode shape function, given by:

$$\boldsymbol{A}_{bf}\ddot{\boldsymbol{x}}_{bf} + \boldsymbol{B}_{bf}\dot{\boldsymbol{x}}_{bf} + \boldsymbol{W}_{bf}(\boldsymbol{x}_{bf}) = \boldsymbol{u}_{bf}(\boldsymbol{u}_b)\ . \tag{5}$$

3.2.2 Motion of the object at the handling point

When the robot is handling the flexible object, vibration of the flexible object is being generated at intermediate points, as well as at the handling points. One purpose in our research is to correspond the endpoints of the robot to any point on the flexible object, and to calculate the respective control input. For the positional constraint requirement, it is difficult to find the relationship at the intermediate point of the object. From this point of view, the state-space equation of the flexible object (eq. (5)) is reduced to neglect the characteristics at all points of the flexible object, except for the handling points. By transforming the state-space variable $\boldsymbol{x}_{bf}$ in eq. (5) into $\boldsymbol{x}_{obr} = [\ x_L\ \ \dot{x}_L\ \ \cdots\ \ \dot{\theta}_L\ \vdots\ x_R\ \ \dot{x}_R\ \ \cdots\ \ \dot{\theta}_R\ ]^T$, the equation of motion of the flexible object at the handling point is given by:

$$\dot{\boldsymbol{x}}_{obr} = \boldsymbol{A}_{obr}\boldsymbol{x}_{obr} + \boldsymbol{B}_{obr}\boldsymbol{u}_{bf}(\boldsymbol{u}_b) + \boldsymbol{W}_{obr}(\boldsymbol{x}_{obr})\ . \tag{6}$$

4 Combined model

4.1 Combined model of the robot and the flexible object

For the combined model consisting of the dual-arm robot and the object, the constraint condition is expressed by using the unknown multiplier method. The combined model can be expressed by combining eq. (1) with eq. (6), using the state-space variable $\boldsymbol{x}_m = [\boldsymbol{\Theta}_L^T\ \boldsymbol{x}_{obr}^T\ \boldsymbol{\Theta}_R^T]^T \in \Re^{o_s\times 1}$. Including the unknown multiplier vector $\boldsymbol{\lambda} \in \Re^{o_c\times 1}$, we get:

$$\dot{\boldsymbol{x}}_m = \boldsymbol{A}_m\boldsymbol{x}_m + \boldsymbol{B}_m\boldsymbol{u}_m + \boldsymbol{W}_m + \boldsymbol{F}_c^T\boldsymbol{\lambda} \tag{7}$$

where $\boldsymbol{u}_m = [\ \boldsymbol{\tau}_L^T\ \ \boldsymbol{\tau}_R^T\ ]^T \in \Re^{o_u\times 1}$ and $\boldsymbol{F}_c = \partial \boldsymbol{f}_c(\boldsymbol{x}_m)\ /\ \partial \boldsymbol{x}_m \in \Re^{o_c\times o_s}$. $\boldsymbol{f}_c(\boldsymbol{x}_m)$ is the vector consisting of the constraint condition which will be noted in the next paragraph. Suppose that the condition rank $\boldsymbol{F}_c = o_c$ has been satisfied. Since $\boldsymbol{B}_m$ includes the Jacobian matrix $\boldsymbol{J}_{aL,R}(\boldsymbol{\theta}_{L,R})$, we suppose the robots move in the region in which the Jacobian matrix is regular.

4.2 Constraint and controllability condition

In this paragraph only, we expand the dual-arm robot case to the general case of m_{ar} arm n_{li} link robot in 2-D space. The constraint condition relating the position of the tip of the robot to the handling point on the object can be expressed by the geometrical relationship depending on the position-posture variable $\boldsymbol{y}$ of the end-effectors and the state-variable $\boldsymbol{x}_{obr}$ of the object. That is to say, the positional constraint condition can be expressed by three kinds of relationship in the state-space $\boldsymbol{x}_m$, *i.e.*, two positional relations in each direction $\boldsymbol{e}_1$ and $\boldsymbol{e}_2$, and the angular relation in the slope of the end-effector and the bending angle among two small elements of the object. (See Figure 4.)

Defining the number of the constraint conditions to be o_c, the constraint force vector is given by:

$$\boldsymbol{f}_c(\boldsymbol{x}_m) \equiv \mathrm{col}(\ f_{c1},\ \ f_{c2},\ \ \cdots,\ \ f_{co_c}\ ) = \boldsymbol{0} \in \Re^{o_c\times 1}\ . \tag{8}$$

The inequality:

$$o_c < o_u \tag{9}$$

is the necessary condition for the combined state-space variable $\boldsymbol{x}_m$ to be controllable by the control input $\boldsymbol{u}_m$. This includes the restriction on the number of conditions to satisfy all the constraint conditions consisting of the element of the state-space $\boldsymbol{x}_m$.

To establish controllability of the flexible object by the robot, let's first consider the relationship between existence of end-effector, and limitation from the inequality condition. (Figure 5.)

If the m_{ar1} arm robot has no end-effector, and the m_{ar2} $(= m_{ar} - m_{ar1})$ arm has end-effectors, among all m_{ar} arm n_{li} link robots, the numbers in the constraint condition (9) are given by:

$$o_c = 3m_{ar} - m_{ar1} , \quad (10)$$

$$o_u = m_{ar}(n_{li} + 1) - m_{ar1} , \quad (11)$$

respectively. From (9), (10) and (11), the following condition is obtained:

$$2 < n_{li} . \quad (12)$$

From eq. (12) we can see that the number (m_{ar}, m_{ar1}, m_{ar2}) of the arms has been neglected and the limitation of the controllability condition does not depend on the existence of the end-effector.

In the particular case of a dual-arm robot with an end-effector, the above condition (eq. (12)) cannot be satisfied. For this reason, we reduce the two constraint conditions imposed from each of the joint angle relationships at both handling points, to one, *i.e.*, the dual-arm robot will not be able to handle either bending angle at the handling point.

4.3 Combined model at the equilibrium point

For the reference posture of the dual-arm robot and the flexible object, define the equilibrium point as $\boldsymbol{x}_m = \boldsymbol{x}_m^*$. Define the notation of the system matrices and vectors at the reference equilibrium point as $(\bullet)^*$. Assume that $\dot{\boldsymbol{\theta}}_{L,R}^* = \ddot{\boldsymbol{\theta}}_{L,R}^* = \mathbf{0}^{3\times 1}$ and $\dot{\boldsymbol{x}}_{obr}^* = \mathbf{0}^{6m_{ar}\times 1}$ hold at the reference equilibrium point. When the constraint condition holds, $\boldsymbol{F}_c^* \dot{\boldsymbol{x}}_m = \mathbf{0}^{o_s\times 1}$ must be satisfied. Consequently, from eq. (7), the reference multiplier vector $\boldsymbol{\lambda}^*$ is obtained. The error motion in the vicinity of the equilibrium point can also be represented by:

$$\Delta\dot{\boldsymbol{x}}_m = \boldsymbol{A}_m^{\sim}\Delta\boldsymbol{x}_m + \boldsymbol{B}_m^*\Delta\boldsymbol{u}_m + \boldsymbol{F}_c^{*T}\Delta\boldsymbol{\lambda} . \quad (13)$$

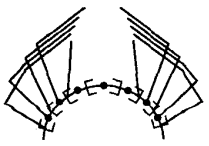

Figure 5: Situation of handling a flexible object by multiple-arm robots.

Notice that matrix $\boldsymbol{A}_m^{\sim}$ is constituted by the static matrix $\boldsymbol{A}_m^*$ and the part of the linearized matrix $\boldsymbol{W}_m^*$. Assume that $(\boldsymbol{A}_m^{\sim}, \boldsymbol{B}_m^*)$ is controllable, and rank $\boldsymbol{B}_m^* = o_u$ is satisfied.

When the constraint condition at the handling points holds, the necessary condition for handling ability is that the equations $\boldsymbol{F}_c^*\Delta\boldsymbol{x}_m = \mathbf{0}^{o_s\times 1}$, $\boldsymbol{F}_c^*\Delta\dot{\boldsymbol{x}}_m = \mathbf{0}^{o_s\times 1}$ must be satisfied. Then the constraint force $\Delta\boldsymbol{\lambda}$ in the vicinity of the reference equilibrium point can also be calculated.

Under the condition that the robots are handling the flexible object perfectly, the equation of the combined model can be expressed by:

$$\Delta\dot{\boldsymbol{x}}_m = \boldsymbol{F}_c^{\sim}\boldsymbol{A}_m^{\sim}\Delta\boldsymbol{x}_m + \boldsymbol{F}_c^{\sim}\boldsymbol{B}_m^*\Delta\boldsymbol{u}_m \quad (14)$$

where $\boldsymbol{F}_c^{\sim} = \boldsymbol{I}^{o_s\times o_s} - \boldsymbol{F}_c^{*T}\boldsymbol{F}_c^{*+} \geq \mathbf{0}^{o_s\times o_s}$, which is a positive semidefinite matrix. For details regarding eq. (14), see [10].

4.4 Stability at the equilibrium point

When the robot has been controlled by the only static equilibrium control input, and has not been controlled by any other control input for stabilization, what happens with the stability condition of the dual-arm robot?

To answer this question, we try to examine the stability of the robot when no control input $\Delta\boldsymbol{u}_m$ at the equilibrium point is applied to the combined model eq. (14).

Since the eigenvalues of matrix $\boldsymbol{F}_c^{\sim}$ are 0 or 1, the condition $\boldsymbol{F}_c^{\sim}\boldsymbol{A}_m^{\sim} \leq \mathbf{0}$ is satisfied if and only if $\boldsymbol{A}_m^{\sim}$ is a negative semidefinite matrix, *i.e.*, $\boldsymbol{A}_m^{\sim} \leq \mathbf{0}$.

1. In case when the internal force at the equilibrium point does not exist, *i.e.*, $\boldsymbol{\lambda}_m^* = \mathbf{0}^{o_c\times 1}$.

   Because $\boldsymbol{A}_m^{\sim}$ is a block diagonal matrix consisting of the system matrices of the robots and the object, the stability of the robots themselfs or the object itself is not collapsed at the equilibrium point if and only if the robots can handle the object perfectly.

2. In case when the internal forces are being generated at the equilibrium point, *i.e.*, $\boldsymbol{\lambda}_m^* \neq \mathbf{0}^{o_c\times 1}$.

   Since $\boldsymbol{A}_m^{\sim}$ includes the vector $\boldsymbol{\lambda}_m^*$, the stability of the system eq. (14) depends upon the value of the static constraint force $\boldsymbol{\lambda}_m^*$.

For the upper two cases, the condition for stability of the system eq. (14) is satisfied if and only if the following holds:

$$\mathcal{S}_m = -\mathrm{Re}\{\lambda_{\max}(\boldsymbol{A}_m^{\sim})\} \geq 0 . \quad (15)$$

5 Handling of the flexible object

5.1 Control system

The necessary condition to realize the handling is to satisfy the constraint condition at the equilibrium point. The state-space of the combined model consists of a sub-space related to the constraint force, and another sub-space which is not involved in any constraints. From this point of view, we consider the decomposition of the state-space model in eq. (14) to constitute a control system for the state-space which is not involved in any constraint force.

Transform the state-space of the combined model eq. (14) as $\Delta\hat{\boldsymbol{x}}_m = \boldsymbol{T}_c^T \Delta\boldsymbol{x}_m$, by a similarity transformation matrix $\boldsymbol{T}_c$. $\Delta\hat{\boldsymbol{x}}_m$ constitutes the unobservable sub-space $\boldsymbol{\mathcal{S}}_{pu}$ and its complement $\boldsymbol{\mathcal{S}}_{po}$. If $(\boldsymbol{A}_m^{\sim}, \boldsymbol{B}_m^*)$ is controllable, then the dimension of the controllable sub-space becomes $\boldsymbol{\mathcal{S}}_{pc} \in \Re^{(o_s - o_c)\times 1}$.

In our formulation, since the dual-arm robot handles the flexible object at the initial time, the boundary condition is satisfied. In other words, because we do not deal with the initial catching of the flexible object here, we do not have to consider the stability of the $\boldsymbol{\mathcal{S}}_{pu}$ sub-space. Since the realization of the cooperative control is possible by stabilizing the $\boldsymbol{\mathcal{S}}_{pc}$ sub-space, we constitute the design of a controller for the $\boldsymbol{\mathcal{S}}_{pc}$ sub-space only. The weighting matrices $\boldsymbol{W}_x \geq \boldsymbol{0}^{(o_s-o_c)\times(o_s-o_c)}$ and $\boldsymbol{W}_u > \boldsymbol{0}^{o_u \times o_u}$ depend upon the state-space in the controllable sub-space $\boldsymbol{\mathcal{S}}_{pc}$ and control input $\Delta\boldsymbol{u}_m$, respectively.

To stabilize the sub-space $\boldsymbol{\mathcal{S}}_{pc}$, we apply the LQ theory minimizing a performance index for the quadratic form which is weighed to the state-space and the control input. Suppose that the system matrices are $(\widehat{\boldsymbol{A}}_{mc}, \widehat{\boldsymbol{B}}_{mc})$ in $\boldsymbol{\mathcal{S}}_{pc}$ sub-space. Using a positive definite solution $\boldsymbol{\Lambda}_{mc}$ of the Riccati equation $\mathrm{REC}(\widehat{\boldsymbol{A}}_{mc}, \widehat{\boldsymbol{B}}_{mc}, \boldsymbol{\Lambda}_{mc})$, the optimal control input for the system eq. (14), in the vicinity of the equilibrium point, is given by:

$$\begin{aligned}\Delta\boldsymbol{u}_m &= [\ \boldsymbol{0}^{o_u \times o_c} \quad -\boldsymbol{W}_u^{-1}\widehat{\boldsymbol{B}}_{mc}^T \boldsymbol{\Lambda}_{mc}\ ]\boldsymbol{T}_c^T \Delta\boldsymbol{x}_m \ . \\ &\equiv \boldsymbol{H}_c \boldsymbol{T}_c^T \Delta\boldsymbol{x}_m \ . \end{aligned} \tag{16}$$

The handling strategy for the flexible object can be achieved using the control input $\Delta\boldsymbol{u}_m$ and the static control input $\boldsymbol{u}_m^*$ at the equilibrium point.

5.2 Stability at the intermediate point of the object

In case of the order o_u of an operation force adds to the robot is restricted, from the condition (9) it is difficult to include the positional relationship at the intermediate point of the flexible object into the constraint condition as eq. (8). This is because the degree of freedom of the flexible object is usually larger than the number o_u of actuators mounted on the robot.

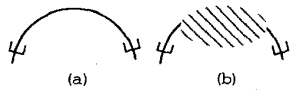

Figure 6: Stability at the intermediate point.

In this paragraph, we examine the characteristics of the flexible object at all points except for the handling point (as shown in Figure 6 (b)), when the control input eq. (16) is applied to the model eq. (14) (as shown in Figure 6 (a)).

We can also examine the response of motion at the intermediate point of the flexible object. Define a new state-space $\Delta\boldsymbol{x}_{m\infty}$ of the combined model consisting of the elements at the intermediate points in the flexible object. Denote the state-space relationship between $\Delta\boldsymbol{x}_m$ and $\Delta\boldsymbol{x}_{m\infty}$ as $\Delta\boldsymbol{x}_m = \boldsymbol{T}_e \Delta\boldsymbol{x}_{m\infty}$ using the transfer matrix $\boldsymbol{T}_e = [\ \boldsymbol{I}^{o_s \times o_s} \ \vdots\ \boldsymbol{0}^{o_s \times (6n_\infty - o_s)}\ ]$, $(n_\infty < \infty)$.

The expanded equation of the combined model at the reference equilibrium point which includes the characteristics at any intermediate point of the object, is given as follows:

$$\Delta\dot{\boldsymbol{x}}_{m\infty} = \boldsymbol{F}_{c\infty}^{\sim}\boldsymbol{A}_{m\infty}^{\sim}\Delta\boldsymbol{x}_{m\infty} + \boldsymbol{F}_{c\infty}^{\sim}\boldsymbol{B}_{m\infty}^*\Delta\boldsymbol{u}_m \ . \tag{17}$$

When the control input eq. (16) is applied to the system eq. (17), the closed loop system is given by:

$$\Delta\dot{\boldsymbol{x}}_{m\infty} = \boldsymbol{F}_{c\infty}^{\sim}(\boldsymbol{A}_{m\infty}^{\sim} + \boldsymbol{B}_{m\infty}^*\boldsymbol{H}_c\boldsymbol{T}_c^T\boldsymbol{T}_e)\Delta\boldsymbol{x}_{m\infty} \ . \tag{18}$$

Concretely, let's examine the stability in the closed loop of the combined model. Taking care that the positional relationship at the intermediate points of the object has not been restricted, $\boldsymbol{F}_{c\infty}^{\sim}$ becomes as follows:

$$\boldsymbol{F}_{c\infty}^{\sim} = \left[\begin{array}{c:c} \boldsymbol{F}_c^{\sim} & \boldsymbol{0} \\ \hdashline \boldsymbol{0} & \boldsymbol{I} \end{array}\right] \ . \tag{19}$$

Noting that $\boldsymbol{F}_{c\infty}^{\sim}$ is a symmetric and positive semidefinite matrix whose eigenvalues are 0 or 1, the necessary condition to satisfy the stability at the intermediate points of the flexible object is given by:

$$\mathrm{Re}\{\lambda_i(\boldsymbol{A}_{m\infty}^{\sim} + \boldsymbol{B}_{m\infty}^*\boldsymbol{H}_c\boldsymbol{T}_c^T\boldsymbol{T}_e)\} < 0 \ \ (\forall\, i\ ) \ . \tag{20}$$

5.3 Robustness of the control system

In the previous paragraph 5.2, we have examined the stability of the flexible object at the intermediate

point except for the handling point.

In the current paragraph, we examine the stability of the handling system (Figure 7 (a)) in case when the object model eq. (6) has uncertainty (Figure 7 (b)), or the handling points are shifted (Figure 7 (c)).

Concretely, assuming that the parameter in the combined model eq. (14) at the reference equilibrium point, is changed as:

$$\boldsymbol{A}_m^{\sim\prime}=\boldsymbol{A}_m^{\sim}(\boldsymbol{I}+\boldsymbol{\Delta}_A),\boldsymbol{B}_m^{*\prime}=\boldsymbol{B}_m^{*}(\boldsymbol{I}+\boldsymbol{\Delta}_B),\boldsymbol{F}_c^{\sim\prime}=\boldsymbol{F}_c^{\sim}(\boldsymbol{I}+\boldsymbol{\Delta}_F), \tag{21}$$

the stability condition can be expressed by the following inequality, using the weighting matrix $\boldsymbol{W}_u$. $\boldsymbol{W}_u$ is used to evaluate the performance index while calculating the control input eq. (16) for the combined model eq. (14), that is:

$$\boldsymbol{\Lambda}_p\boldsymbol{W}_u^{-1}+\boldsymbol{W}_u^{-1}+\boldsymbol{W}_u^{-1}\boldsymbol{\Lambda}_p^T\geq\boldsymbol{0} \tag{22}$$

where

$$\begin{aligned}\boldsymbol{\Lambda}_p=&\boldsymbol{\Delta}_B+\boldsymbol{B}_m^{*+}\boldsymbol{\Delta}_F\boldsymbol{B}_m^{*}(\boldsymbol{I}+\boldsymbol{\Delta}_B)\\&-\boldsymbol{B}_m^{*+}(\boldsymbol{\Delta}_F\boldsymbol{A}_m^{\sim}+\boldsymbol{\Delta}_F\boldsymbol{A}_m^{\sim}\boldsymbol{\Delta}_A+\boldsymbol{A}_m^{\sim}\boldsymbol{\Delta}_A)(\boldsymbol{H}_c\boldsymbol{T}_c^T)^+.\end{aligned} \tag{23}$$

For this calculation, we utilized the theory in [12] with some modification. If the weighting matrix $\boldsymbol{W}_u$ in (22) is symmetric, the condition of (22) can be reformulated:

$$\mathcal{S}_\delta=\mathrm{Re}\{\lambda_{\min}(\boldsymbol{\Lambda}_p\boldsymbol{W}_u^{-1}+\boldsymbol{W}_u^{-1}+\boldsymbol{W}_u^{-1}\boldsymbol{\Lambda}_p^T)\}\geq 0\ . \tag{24}$$

Using the above inequalities (22), (24), we can examine the stability of the handling model eq. (14) for the uncertainty of the physical characteristics, and for the change of the handling points. In case when the handling points are changed, note that both the characteristics of the object and $\boldsymbol{F}_c^{\sim}$ are changed, respectively.

1. In case of the characteristics of the flexible object being changed:

$$\boldsymbol{A}_m^{\sim}\rightarrow\boldsymbol{A}_m^{\sim\prime},\ \boldsymbol{B}_m^{*}\rightarrow\boldsymbol{B}_m^{*\prime},\ \boldsymbol{F}_c^{\sim}\rightarrow\boldsymbol{F}_c^{\sim}\ . \tag{25}$$

2. In case of the handling points being changed:

$$\boldsymbol{A}_m^{\sim}\rightarrow\boldsymbol{A}_m^{\sim\prime},\ \boldsymbol{B}_m^{*}\rightarrow\boldsymbol{B}_m^{*\prime},\ \boldsymbol{F}_c^{\sim}\rightarrow\boldsymbol{F}_c^{\sim\prime}\ . \tag{26}$$

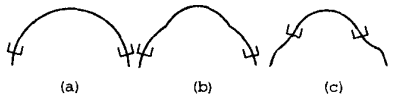

Figure 7: Change of the model and the handling point.

Re-writing the matrix form as above, calculating eq. (23), and substituting eq. (23) into (22) or (24), the handling system for the flexible object becomes stable, if the condition forms (22) or (24) are satisfied.

6 Simulation

We present simulation results of the proposed handling system for a flexible object using a rigid dual-arm robot. We set the posture of two robots as reference considering the bending of the flexible object as zero. Thus we set the static control input $\boldsymbol{u}^*$ as the value obtained from the condition that the bending of the flexible object is zero. To understand the stability and the robustness of our handling system, we examine the bending displacement of the object in y-axis, while holding the bending in x-axis to zero. This we do because the parameters of the stability and robustness conditions increase and the analysis becomes more complex than that in 1-D space. A simulation study has been carried out for the combined model eq. (14), for two different reference postures: (A) when both the bending displacement of the flexible object and each of the joint angles are equal to zero, and (B) both the bending displacement of the flexible object and the joint velocity of each robot equal to zero. It is possible to control the flexible object using the control input $\boldsymbol{\Delta u}_m$ in the vicinity of the equilibrium point and the static control input $\boldsymbol{u}_m^*$ at the equilibrium point. The dynamic behavior of the combined model eq. (14) is computed by the fourth order Runge-Kutta method.

Figure 8 shows the stability of the combined model eq. (14) for the parameter change of the flexible object when the robot has been controlled by the only static equilibrium control input. The value of $\mathcal{S}_m$ in eq. (15) is plotted in Figure 8. In Figure 8, the area in which the value of $\mathcal{S}_m$ is positive, is stable for the parameter change of the object at the equilibrium point. On the contrary, if the value of $\mathcal{S}_m$ is negative, the combined model eq. (14) is unstable. The part in which the value of $\mathcal{S}_m$ is zero stands for case when the combined model eq. (14) has vibratory characteristics. The dashed line stands for the characteristics of the object when the control input eq. (16) is applied to the combined model eq. (14).

Figures 9, 10 show the responses of the combined model eq. (14) when the characteristics of the object are changed. Figure 9 shows the bending displacement of the object when the object is stable (in the case of eq. (15) being satisfied, and $\mu A_\rho = 0.80$ [Ns/m] in Figure 8). Figure 10 shows the bending displacement when the object is unstable (in the case of eq. (15)

being not satisfied, and $\mu A_\rho = 0.10$ [Ns/m] in Figure 8). Figure 10 shows that the vibration has been also generated.

Figure 11 shows the bending displacement of the object when the control input eq. (16) is applied to the combined model eq. (14). At that time, Figure 12 shows the responses of the joint angles of each robot (eq. (1)). Figure 13 shows the static control input $\boldsymbol{u}_m^*$ at the equilibrium point (as shown by straight lines), and the control input $\boldsymbol{\Delta u}_m$ in the vicinity of the equilibrium point (as shown by curved lines).

Figure 14 shows the responses of the bending displacement at the intermediate points $\Delta y_{2,\,3,\,4} = 0.25L,\ 0.50L,\ 0.75L$, where L stands for the link length. We can see that the stabilization is achieved with LQR robustness.

Figure 15 shows the bending displacement of the object when the regulated static control input $\boldsymbol{u}_m^*$ is also applied to the combined model eq. (14) to compensate the steady-positional-state error, in the period from 1.0 [s] to 1.5 [s]. At that time, Figure 16 shows the responses of the joint angle of each robot (eq. (1)).

Next, we examine the robustness of the controller eq. (16). Figure 17 shows the stability of the combined model eq. (14) controlled by eq. (16) in the vicinity of the nominal characteristics ($\mu A_\rho = 0.15$ [Ns/m]) of the flexible object. The value of $\mathcal{S}_\delta$ in (24) is plotted in Figure 17. If the area in which the value of $\mathcal{S}_\delta$ is positive, then the closed loop of the combined model eq. (14) is stable, while when the value is negative, then the combined model is unstable. From Figure 17, we can see that the stable area is 0.14 [Ns/m] $\leq \mu A_\rho \leq 0.165$ [Ns/m]. Figures 18, 19 are the responses of the bending displacement of the object at the handling point in the neighborhood of the stability limitation. Figure 18 shows the responses in the stable side ($\mu A_\rho = 0.145$ [Ns/m]), Figure 19 shows the responses in the unstable side ($\mu A_\rho = 0.13$ [Ns/m]).

Figures $20 \sim 23$ show the stability of the combined model eq. (14) when each of the handling points are changed. Figure 20 shows the stability of the combined model eq. (14) for the change of the handling point x_R at right side, using the controller eq. (16) derived for the handling point $x_L = 0.05L$ [m], $x_R = 0.95L$ [m]. Figure 21 shows an enlargement at the stability limitation in Figure 20. We can see that the stability area is $0.92L$ [m] $\leq x \leq 0.98L$ [m]. Figures 22, 23 show the responses of the bending displacement at the handling point in the neighborhood of the stability limitation. Figure 22 shows the responses of the bending displacement when the value $\mathcal{S}_\delta$ is in the stable area ($x = 0.93L$ [m]), while Figure 23 shows the responses when the values of the combined model eq. (14) is in the unstable area ($x = 0.91L$ [m]).

Figures 24, 26 and 28 show the situations of the handling of the flexible object by the dual-arm robot, in which the damping force coefficient μ of the object is changed. Both robots are being fixed in the positions $(0, 0)$ and $(5, 0)$. Figures 25, 27 and 29 show the trajectory of some points on the object. Figures 24, 25 show the vibration control of the object in narrow space. Figures 26, 27 show the situation of position control of handling points when the robots move in narrow space. Figures 28, 29 show the deformation control in large space and in the case when the physical parameter μ is changed. In Figure 28, since the internal force in eq. (7) exceeds the value ($\max \boldsymbol{\lambda}_m = 10.0$) decided in advance, the hands of the dual-arm robot are separated from the object, in the middle of the handling.

7 Conclusions

We have proposed a handling system for a flexible object, that is changing its form transforming in 2-D space, using rigid arm robots. For this strategy, we have constituted the combined model which consists of the robots and the flexible object to make the whole handling system stable. We have also designed the controller to satisfy the stability of the handling system, and have analyzed the stability of the controller at the intermediate points of the flexible object. Furthermore, we have found the robust handling condition. In the numerical simulation, we have recognized that our handling system can be applied for position control of the flexible object by the rigid robots.

In our future work, we would like to find the limitation of the handling tasks for the flexible object by the robot, mathematically.

In future, we plan also to have experiments.

References

[1] M. Uchiyama and P. Dauchez: A symmetric hybrid position/force control scheme for the coordination of two robots., Proc. of IEEE Int. Conf. on Robotics and Automation, pp. 350–356, 1988

[2] H. Nakagaki, K. Kitagaki and H. Tsukune: Study of insertion task of a flexible beam into a hole., Proc. of IEEE Int. Conf. on Robotics and Automation, Vol. 1, pp. 330–335, 1995

[3] T. Yukawa, M. Uchiyama and H. Inooka: Handling of a constrained flexible object by a robot., Proc. of IEEE Int. Conf. on Robotics and Automation, Vol. 1, pp. 324–329, 1995

[4] Y. F. Zheng and M. Z. Chen: Trajectory planning for two manipulators to deform flexible beams., Proc. of IEEE Int. Conf. on Robotics and Automation, pp. 1019–1023, 1993

[5] Omar Al-Jarrah, Y. F. Zheng and Keon-Young Yi: Efficient trajectory planning for two manipulators to deform flexible

materials with experiments., Proc. of IEEE Int. Conf. on Robotics and Automation, Vol. 1, pp. 312–317, 1995

[6] Omar Al-Jarrah, Y. F. Zheng and Keon-Young Yi: Trajectory planning for two manipulators to deform flexible materials using compliant motion., Proc. of IEEE Int. Conf. on Robotics and Automation, Vol. 2, pp. 1517–1522, 1995

[7] K. Kosuge, M. Sakai and K. Kanitani: Manipulation of a flexible object by dual manipulators., Proc. of IEEE Int. Conf. on Robotics and Automation, Vol. 1, pp. 318–323, 1995

[8] M. M. Svinin and M. Uchiyama: Cartesian-level control strategy for a system of manipulators coupled through a flexible object., Proc. of IEEE/RSJ/GI Int. Conf. on Intelligent Robots and Systems, Vol. 1, pp. 687–694, 1994

[9] M. M. Svinin and C. von Albrichsfeld: Analysis of constrained elastic manipulations., Proc. of IEEE/RSJ Int. Conf. on Intelligent Robots and Systems, Vol. 2, pp. 414–421, 1995

[10] T. Yukawa, M. Uchiyama and H. Inooka: Cooperative control of a vibrating flexible object by a rigid dual-arm robot., Proc. of IEEE Int. Conf. on Robotics and Automation, Vol. 2, pp. 1820–1826, 1995

[11] J. C. Simo and L. Vu-Quoc: On the dynamics of flexible beams under large overall motions—The plane case: Part I and Part II., Trans. ASME, J. of Applied Mechanics, Vol. 53, Dec., pp. 849–863, 1986

[12] M. G. Safonov and M. Athans: Gain and phase margin for multiloop LQG regulators., IEEE Trans. Automat. Contr. Vol. AC-22, pp 173–179, 1977

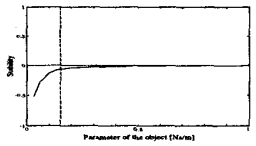

Figure 8: Stability bounds.

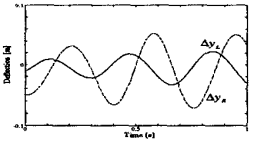

Figure 9: Bending displacement.

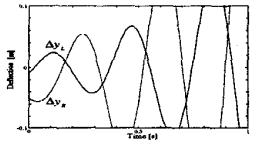

Figure 10: Bending displacement.

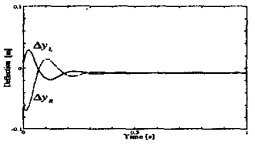

Figure 11: Bending displacement.

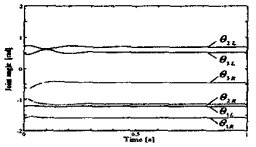

Figure 12: Joint angle of the robot.

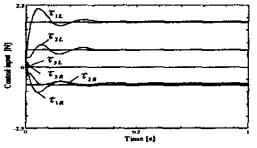

Figure 13: Control input in the vicinity of the equilibrium point.

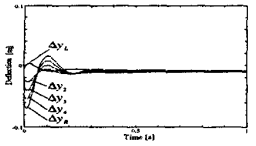

Figure 14: Responses at the intermediate point of the object.

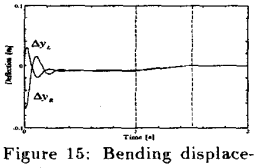

Figure 15: Bending displacement.

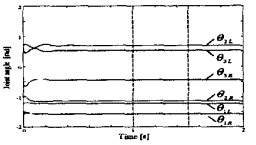

Figure 16: Joint angle of the robot.

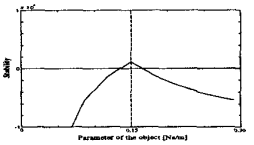

Figure 17: Stability bounds.

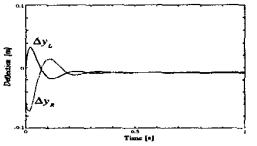

Figure 18: Bending displacement.

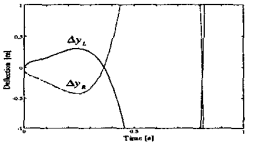

Figure 19: Bending displacement.

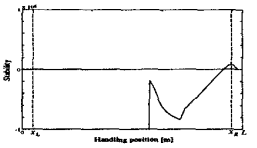

Figure 20: Stability bounds.

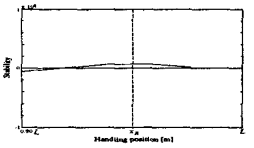

Figure 21: Stability bounds. (an enlargement)

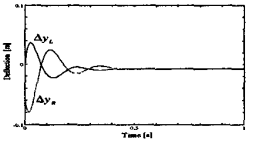

Figure 22: Bending displacement.

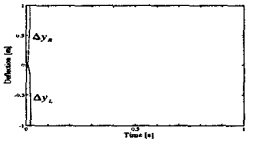

Figure 23: Bending displacement.

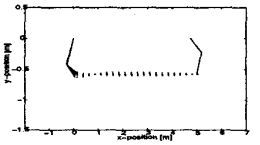

Figure 24: Situation of the handling. ($\mu = 1.00$).

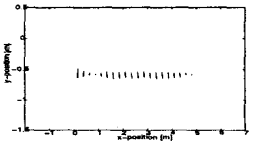

Figure 25: Trajectory of the object. ($\mu = 1.00$).

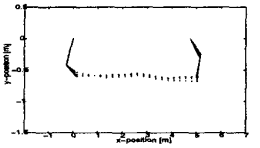

Figure 26: Situation of the handling. ($\mu = 1.00$).

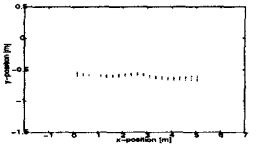

Figure 27: Trajectory of the object. ($\mu = 1.00$).

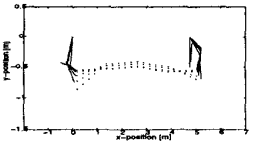

Figure 28: Situation of the handling. ($\mu = 10.00$).

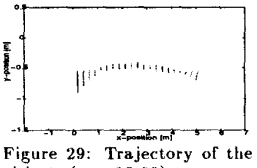

Figure 29: Trajectory of the object. ($\mu = 10.00$).